



Estimation of Waste Heat from Exhaust Gases of an Iron Ore Pelletizing Plant in Iran

S. Goodarzi¹, E. Jahanshahi Javaran^{1*}, M. Rahnama², M. Ahmadi³

¹ Department of Energy, Institute of Science and High Technology and Environmental Sciences, Graduate University of Advanced Technology, Kerman, Iran

² Mechanical Engineering Department, Faculty of Engineering, Shahid Bahonar University of Kerman, Kerman, Iran

³ Golgohar Iron Ore and Steel Research Institute, Golgohar Mining and Industrial Company, Sirjan, Iran

ABSTRACT: Waste heat from the exhaust gases of Golgohar iron ore pelletizing Plant, in Sirjan, Iran, was studied using energy analysis based on input data extracted from measurements in a 5-month period. Constituents considered as inputs were fresh air, natural gas, green and indurated pellets, while the exhaust flue gas and hot indurated pellets were served as the output. Contribution of each part to energy production and/or consumption was separately determined, in addition to the energy produced from burning of natural gas and pyrite and magnetite oxidation to hematite. Special consideration was devoted to the energy leaving the furnace through exhaust flue gases as the main source of waste heat in addition to the latent heat of water vapor, the energy stored in materials such as indurated pellets, rail pallets and cooling water, and radiation from the furnace body. It was observed that the dominant portion of waste heat is in the form of thermal energy carried by flue gases generated from combustion which are released into the atmosphere. The present study can be considered as a case study for a specific plant which gives insights on how to handle and analysis the waste heat recovery of such plans in general.

Review History:

Received: 1 March 2018

Revised: 30 July 2018

Accepted: 30 July 2018

Available Online: 18 August 2018

Keywords:

Green pellet

Energy analysis

Flue gas

Induration furnace

Indurated pellet

1- Introduction

Waste heat is defined as the heat produced in a fuel combustion process or chemical reactions, which enters into the environment in the absence of the proper means to recovery it. Waste heat recovery has always been a subject of interest in various industries due to such advantages as reducing the amount of fossil fuels consumption and their subsequent greenhouse gas emissions and producing the final product at a lower price. Evaluation of the waste heat potential can be performed through the study scale and/or data acquisition, each with a bottom-up or top-down approach. In a recent work, Brückner et al. [1] classified and compared different methods of estimating the industrial waste heat recovery. It can also be considered from another viewpoint in which theoretical, technical and economic potentials are investigated [2].

As the main step in estimating the amount of recoverable energy, analysis of mass and energy balance should be done for the desired process. Iron ore pelletizing plants are among the energy-intensive processes in steel industry with the potential of producing a substantial amount of waste heat. Waste heat from such pelletizing plants is the part of heat produced in the oxidization of pellets. The induration process of a single pellet in a travelling grate furnace was investigated by Vitoretti and Costo [3] to obtain temperature distribution within pellets during the induration phenomenon. In their study, mass, momentums and energy transfer between pellets and gas were taken into account, while the focus of their work was on the firing phenomenon to establish a mathematical model

Corresponding author, E-mail: e.jahanshahi@kgut.ac.ir

describing each phase and chemical species. It was concluded that pellets with a narrow distribution resulted in the proper inner temperature gradient, thereby improving metallurgical and mechanical properties. A simulation known as the virtual induration of wet iron ore pellets on a moving grate of an iron pelletizing plant was presented by Majumder et al. [4]. In their study, numerous parameters were used as the input for the model; these included temperature and composition of the inlet gas, the moisture content of wet pellets and their mean diameters, the temperature profile of firing hood, hearth layer heights, pellet bed and grate length. Their numerical solution of transient mass and energy conservation equations was obtained using a software tool capable of improving the productivity of furnace, optimizing fuel cost, and serving as a simulator of the operator's training. The outcomes of the simulation tool were composition profiles, gas temperature, burn-through point temperature and its location. In another work, Barati [5] simulated the process of pellet induration in a straight-grate system dynamically, considering the effect of pellet porosity and bed shrinkage. In addition, the influence of physical and chemical phenomena on the heat and mass transfer analysis was taken into account in their mathematical modeling. Their proposed model was validated through comparison of the computational results with the actual measurements of the industrial and pilot-scale plants. Their study helped to understand the process details, resulting in a useful tool for furnace designing and process optimization. Some authors have considered the optimization of parameters affecting the pelletizing process. In a simulation study by Feng et al. [6], the influential parameters of preheating process

and pellet drying in a grate induration furnace of the pellet production process were optimized. Their results showed that an increase in the efficiency of drying and preheating process could occur with the higher wind temperature and velocity, and the lower material thickness and initial moisture.

Nordgren et al. [7] analyzed mass and energy flows through the straight grate induration furnace of an iron-ore pelletizing plant in MalMBERGET. The aim of their study was to establish a framework for mass and energy balances in the whole process and also, to optimize the environmental impacts and energy consumption. This analysis provided a basis for the total mass and energy balances in the entire production chain. Some mathematical modeling of an industrial-scale iron ore pellet induration process which considered mass, heat and momentum transfers was carried out by Sadrnezhaad et al. [8]. In this model, variations of gas composition through the furnace, gas concentration change from one step to another one, temperature distribution in the pellets, and geometry effects were investigated. The results of this analysis showed the sensitivity of process to the operating conditions. Feng et al. [9] also developed a mathematical model for the drying and preheating phenomena of iron ore pellets in a traveling grate based on mass, momentum and heat transfer laws, and semi-empirical correlations. The effect of the pertinent parameters including the mean diameter of pellets, the grate velocity, the initial moisture and the inlet gas temperature on the temperature profile of pellets was investigated through the traveling grate. It was shown that increasing the pellet mean diameter resulted in raising the bed temperature in the drying zone. The reverse phenomenon took place in the preheating zone. Also, they mentioned that the lower initial moisture resulted in economizing the energy usage.

As is observed from above-mentioned literature survey, most of the previous studies regarding pellet induration furnaces are based on mathematical modeling applying mass and energy balance and physical-chemical reaction equations to reveal the effect of parameters such as temperature and reaction rates on the process in the pellet induration phenomenon and its optimization. To the best of author's knowledge, there is no published work revealing waste heat potential of a pelletizing plant through mathematical modeling and experimental data, especially for the heat which might be recovered in ducts and/or main stack of the plant. In the present study, mass and energy flow analysis of Golgohar iron ore pelletizing plant, located in Sirjan, Iran, was performed using the measured data for a period of five months of plant operation. This plant, which is the largest energy consumer of Golgohar Mining and Industrial Company, is of prime importance from an energy efficiency view point. The origin of energy production in this plant is from the burning of natural gas, released energy due to the conversion of magnetite to hematite, and pyrite burning of the inlet green pellets. Part of the energy produced in the induration furnace is released in to the atmosphere by flue gases flowing through three ducts connected to the main stack, each with different compositions and temperatures. Stored energy in the indurated pellets, grate bars and cooling water around the furnace body, and the emitted radiation from the furnace body with different temperatures are among other sources of waste heat. It should be mentioned that the most important contribution to the exhaust energy of the furnace is in the form of the sensible heat of the flue gas and the latent heat of the water vapor inside. In the following sections, the

process in the Golgohar iron ore pelletizing Plant, which includes induration furnace and process principles, is first presented, followed by the mathematical modeling of the process and the results and discussion section. Finally, the last part is devoted to the concluding remarks.

2- Plant Description

Golgohar iron-ore pelletizing plant is part of Golgohar iron-ore Company which is located at a distance of 60 km in the west of Sirjan, in Kerman province, Iran. This plant was designed for an annual production capacity of five million tons of indurated pellets [10]. Iron-ore pellets in the form of spheres are produced from the agglomeration of iron-ore concentrates. Straight grate indurating machine is used for the induration of the pellets. The induration area has been designed as a traveling grate method. Under normal operating conditions, the speed of the grate is about 3.6 to 4.4 m/min. The induration machine is a closed chain of 232 pallets, each having 4 m width, 1.5 m length and 10000 kg weight, providing a total area of 624 m². Fig. 1 shows a schematic representation of the iron-ore straight grate induration furnace [10]. The action of the sensor shown in this figure is described in the legend of this figure.

Six process gas fans are installed to maintain the required gas flow for the indurating machine [11]. Process fans include: Exhaust fans: G5.042, G5.036, and G5.037, Recuperation fan: G5.022, Up-draught drying fan: G5.012, and cooling air fan: G5.002. Cooling air system represents the main intake of the ambient air into the indurating machine. Ambient air is supplied to the cooling zone of the indurating machine by G5.002 fan and is used to cool down the indurated pellets. Exhaust gas (hot ambient air at a temperature of approximately 315°C) is taken from the hood of the 2nd cooling zone by the G5.012 fan and supplied to the windboxes of the up-draught drying zone which is used for the initial drying of the green pellets. The process gases from parts of the firing and after firing zones are taken by the G5.022 recuperation fan and used for the drying of green pellets in the down-draught drying zone. Three fans including G5.042, G5.036 and G5.037 are used to exit the exhaust gases from the up-draught, down-draught and preheating zones to the main stack, respectively.

3- Mathematical Modeling of the Process

By considering a control volume around the induration furnace, mass and energy conservation equations were written for a steady state inflow/outflow of gas and solid phases. Fig. 2 shows a schematic of the control volume around the induration furnace and its mass inflow/outflow.

All abbreviations observed in Fig. 2 are defined in the Nomenclature. It is worth mentioning that the control volume was chosen such that its boundaries would cross the entrance of each duct (G5.036, G5.037 and G5.042), not including the volume of the main stack. This was due to different energy qualities existing in each duct, a parameter depending on the temperature and flue gas components.

Assumptions considered in the present analysis are mentioned here:

- Sensible energy required to raise the water temperature in the pellets to the boiling point is ignored,
- There is no air leakage from and air inspiration inside the furnace,
- Dust plays no role in the mass and energy analysis,

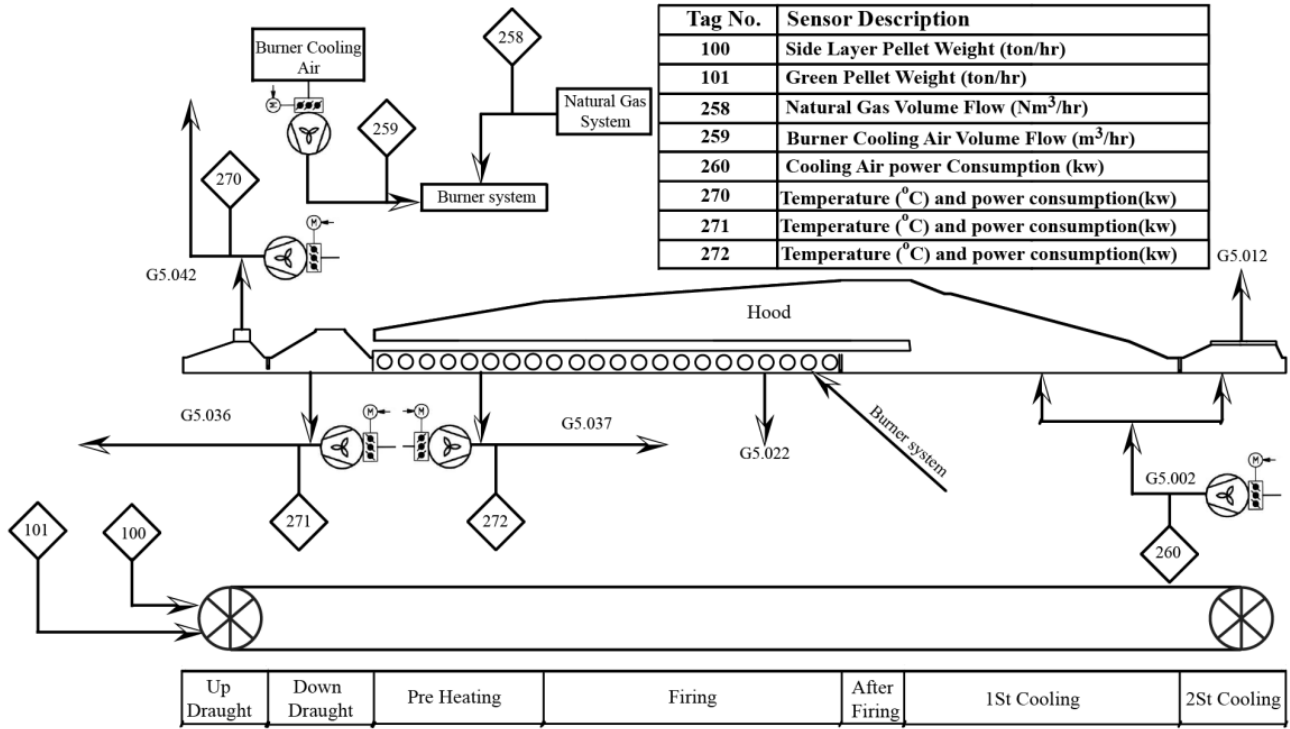


Fig. 1. A schematic representation of the iron-ore straight grate induration furnace under consideration.

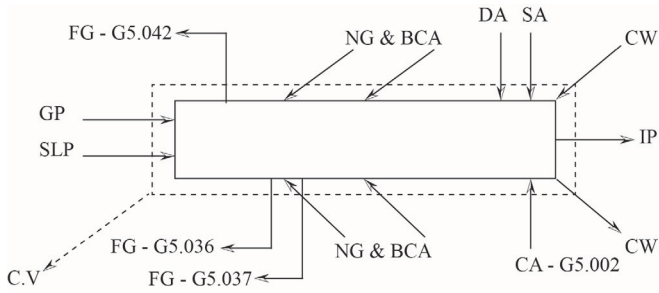


Fig. 2. Schematic of control volume around the induration furnace and its mass inflow/outflow.

- Reference temperature considered as the dead state is selected as 20°C; it is the average temperature of air for an interval of 5 months from 21 March 2015 to 22 August 2015, at the plant location.

3- 1- Mass balance

For a steady flow situation, the mass balance equation is simply expressed as [12]:

$$\dot{m}_{in} = \dot{m}_{out} \quad (1)$$

The inlet mass flow rates include fresh air (\dot{m}_a), natural gas (\dot{m}_{NG}) and the solid phase containing both green (\dot{m}_{GP}) and indurated pellets used as the side layer pellet (\dot{m}_{SLP}), which can protect the grate bar from overheating, etc. Outflow includes the exhaust flue gas (\dot{m}_{FG}) and indurated pellets (\dot{m}_{IP}). Due to chemical reactions and the combustion occurring inside the furnace, flue gases contained gases formed during the reaction in addition to the fresh air entering into the furnace. By considering constituent components, the mass balance can be rewritten as [11]:

$$\dot{m}_a + \dot{m}_{NG} + \dot{m}_{GP} + \dot{m}_{SLP} = \dot{m}_{FG} + \dot{m}_{IP} \quad (2)$$

Four parts of the fresh air, \dot{m}_a , are:

- Sealing air (\dot{m}_{SA}): In two zones of the induration furnace, i.e. up-draught and second cooling, the positive pressure exists, causing hot gases to escape from the furnace. To prevent this phenomenon, some fresh air known as sealing air is injected into the furnace.
- Dilution air (\dot{m}_{DA}): If the temperature of gases passing through two process fans of G5.012 and G5.022 exceeds the design temperature, an air stream known as dilution air is injected upstream of these process fans.
- Burner combustion air (\dot{m}_{BCA}): The air required for the combustion of natural gas.
- Cooling air (\dot{m}_{CA}): The air required for the cooling of the indurated pellets.

Therefore, the inflow fresh air is expressed as [11]:

$$\dot{m}_a = \dot{m}_{SA} + \dot{m}_{DA} + \dot{m}_{BCA} + \dot{m}_{CA} \quad (3)$$

To protect pellets from heat, the hearth- and side layer consisting of indurated pellets was screened off from production and circulated back to the hearth- and side layer; bins were fed to the indurating machine feed area [11]. The indurated pellets used as the hearth- and side layer did not have any chemical reaction; their role in energy balance was to bring out some energy from the furnace. Inlet green pellets had different weights, as compared to those of indurated pellets. This was due to loss of sulfur and water in the induration process and also, the oxygen added for the conversion of magnetite to hematite (FeO) and pyrite burning. During the induration process in the furnace, the water content of green pellets was vaporized in the up-draught, down-draught and

beginning of the pre-heating stages. In order to calculate the weight percentage of water content in green pellets, samples of inlet green pellet to the furnace were examined four times during each day. Then, these samples were ground and heated to vaporize water, resulting in the dry pellets. The weight of the water content of green pellets could be obtained from the difference in the weight of dry and green pellets. Hence, the mass flow rate of dry pellets (\dot{m}_{DP}) could be calculated by Eq. (4) [11].

$$\dot{m}_{DP} = \dot{m}_{GP} (1 - \text{Water Content} (\%)) \quad (4)$$

The sulfur content of the pellets was reduced in furnace due to its reaction with oxygen and production of SO_2 . The weight percentage of sulfur and magnetite inside the pellets was examined in laboratory four times during each day. The amount of oxygen added to the pellets during the pellet induration (conversion of magnetite to hematite) could be computed from its reaction equation, i.e. $4(\text{Fe}_2\text{O}_3 \cdot \text{FeO}) + \text{O}_2 \rightarrow 6\text{Fe}_2\text{O}_3$. Based on the aforementioned issues, the mass flow rate of the indurated pellets (\dot{m}_{IP}) could be obtained as Eq. (5) [11].

$$\dot{m}_{IP} = \dot{m}_{DP} (1 - \text{Sulphur Loses} (\%) + \text{Oxygen Added} (\%)) \quad (5)$$

The added mass (\dot{m}_{Added}) as a portion of the flue gases could be obtained as Eq. (6) [11].

$$\begin{aligned} \dot{m}_{Added} &= \dot{m}_{GP} \times \text{Water Content} (\%) \\ + \dot{m}_{DP} \times (\text{Sulphur Loses} (\%) - \text{Oxygen loses} (\%)) \end{aligned} \quad (6)$$

On the other hand, the weight of indurated pellets changes as a result of releasing their water content through evaporation, in addition to the oxidization of sulfur and some added oxygen. As will be shown later, the difference between the mass flow rate of the pellets entering into and that exiting from the furnace is about two percent of the inlet mass flow rate considered as part of the mass of flue gases. The exit mass flow rate of flue gases (\dot{m}_{FG}) from the main stack is composed of that flowing in three ducts of G5.036, G5.037 and G5.042 [11]:

$$\dot{m}_{FG} = \dot{m}_{G5.036} + \dot{m}_{G5.037} + \dot{m}_{G5.042} \quad (7)$$

Here, $\dot{m}_{G5.036}$, $\dot{m}_{G5.037}$ and $\dot{m}_{G5.042}$ are the mass flow rates corresponding to each duct. It should be mentioned that these ducts contain gases with different chemical compositions due to their placement at different locations.

3- 2- Energy Balance

The steady state energy balance is expressed as [12]:

$$\dot{E}_{in} + \dot{E}_{gen} = \dot{E}_{out} \quad (8)$$

The amount of the energy entering into the furnace, \dot{E}_{in} , is related to fresh air (\dot{E}_a), natural gas (\dot{E}_{NG}), green pellets (\dot{E}_{GP}), and side layer pellets (\dot{E}_{SLP}), as follows [11]:

$$\dot{E}_{in} = \dot{E}_a + \dot{E}_{NG} + \dot{E}_{GP} + \dot{E}_{SLP} \quad (9)$$

in which, [11, 12]:

$$\dot{E}_a = \dot{m}_a C_{p,a} (T_a - T_{Ref}) \quad (10)$$

$$\dot{E}_{NG} = \dot{m}_{NG} C_{p,NG} (T_{NG} - T_{Ref}) \quad (11)$$

$$\begin{aligned} \dot{E}_{Inlet\ Pellet} &= \dot{E}_{GP} + \dot{E}_{SLP} \\ &= (\dot{m}_{GP} + \dot{m}_{SLP}) C_{p, Iron\ Pellet} (T_{Inlet\ Pellet} - T_{Ref}) \end{aligned} \quad (12)$$

It should be noted that all these energies are calculated with reference to the ambient temperature, which is considered as the dead state. As fresh air (T_a) and natural gas (T_{NG}) are at the ambient temperature (T_{Ref}), the inlet energy to the furnace by fresh air (\dot{E}_a) and natural gas (\dot{E}_{NG}) can be ignored. $T_{Inlet\ Pellet}$ is the weighted-average temperature of green and side layer pellets, to be described in the Results section.

Three mechanisms for heat generation comprise the combustion of natural gas, the conversion of magnetite to hematite and pyrite burning, which are expressed as [11]:

$$\dot{E}_{gen} = \dot{E}_{NG} + \dot{E}_{Feo} + \dot{E}_{Pyrite} \quad (13)$$

Using heat of reaction, each of these energy generations can be obtained from the following relation [12]:

$$\dot{E}_{Reaction} = \dot{m}_{Reaction} \times \Delta H \quad (14)$$

This thermal energy, which leaves the induration furnace, is composed of the heat of flue gases (sensible, \dot{E}_{FG}), the latent heat of the water vapor (\dot{E}_{WV}) flowing in three ducts, energy storage by indurated pellets (\dot{E}_{IP}), pallets (\dot{E}_{Pallet}) and cooling water (\dot{E}_{CW}), emitted radiation from the furnace body (\dot{E}_{Rad}), and other losses ($\dot{E}_{Other\ Losses}$), as described below [11]:

$$\begin{aligned} \dot{E}_{out} &= \dot{E}_{FG} + \dot{E}_{WV} + \dot{E}_{IP} + \dot{E}_{Pallet} \\ &+ \dot{E}_{CW} + \dot{E}_{Rad} + \dot{E}_{Other\ Losses} \end{aligned} \quad (15)$$

Sensible energy transferred by flue gases at three ducts can be obtained from the following equation [11]:

$$\dot{E}_{FG} = \dot{E}_{G5.036} + \dot{E}_{G5.037} + \dot{E}_{G5.042} \quad (16)$$

in which [12]:

$$\dot{E}_{G5.036} = \dot{m}_{G5.036} C_{p,G5.036} (T_{G5.036} - T_{Ref}) \quad (17-a)$$

$$\dot{E}_{G5.036} = \dot{m}_{G5.037} C_{p,G5.037} (T_{G5.037} - T_{Ref}) \quad (17-b)$$

$$\dot{E}_{G5.036} = \dot{m}_{G5.042} C_{p,G5.042} (T_{G5.042} - T_{Ref}) \quad (17-c)$$

The energy carried by water vapor at three ducts can be calculated by [12]:

$$\dot{E}_{WV} = \dot{m}_{WV} \times H_{fg} \quad (18)$$

where H_{fg} is the enthalpy of water vaporization.

Thermal energy leaving the induration furnace by the indurated pellets is obtained as [12]:

$$\dot{E}_{IP} = \dot{m}_{IP} C_{p, Iron Pellet} (T_{IP} - T_{Ref}) \quad (19)$$

Thermal energy absorbed by cooling water in the jackets of the furnace is obtained from [12]:

$$\dot{E}_{CW} = \dot{m}_{CW} C_{p, CW} \Delta T \quad (20)$$

In the above equation, ΔT is the temperature difference between the inlet and outlet cooling water. Waste heat from the conveyer (pallet rail) to the ambient temperature is obtained as follows [12]:

$$\dot{E}_{Pallet} = \dot{m}_{Pallet} C_{p, Pallet} \Delta T \quad (21)$$

There is waste heat by radiation from the furnace envelope, depending on its area and temperature, outside air temperature, wind speed and surface emissivity. A correlation proposed for estimating such waste heat is expressed as [13, 14]:

$$\dot{E}_{Rad \& conv} \text{ (Btu/hr)} = \left[\begin{array}{l} 0.174 \times 10^{-8} \varepsilon [T_{Sur}^4 - T_a^4] + \\ 0.296(T_{Sur} - T_a)^{1.25} \sqrt{\frac{(V_{Wind} + 69)}{69}} \end{array} \right] A_{Sur} \text{ (ft}^2\text{)} \quad (22)$$

Please note that area is in ft² and temperatures are in Rankin in the above equation. Wind speed is neglected here as the induration furnace is located in an enclosed area.

3-3- The calculation method

In this study a FORTRAN code was developed to solve the set of mass and energy balance equations. The solution strategy could be briefly described as follows:

I. Mass balance

All mass flow rates are obtained from laboratory results or measurements by sensors and measuring devices.

- \dot{m}_a in Eq. (2) consists of four terms; \dot{m}_{SA} , \dot{m}_{DA} , \dot{m}_{BCA} , and \dot{m}_{CA} . Each of these terms as well as \dot{m}_{FG} is obtained from characteristic curves, the opening percentage of the damper, and the power consumption of the corresponding fans.
- \dot{m}_{NG} in Eq. (2) is measured by the metering device installed in the plant.
- The difference between the weight of sulfur (Pyrite) and magnetite (FeO) in green and indurated pellets is equal to the weight of burned sulfur and magnetite in the process respectively.
- Measured values of \dot{m}_{GP} and \dot{m}_{SLP} by the sensors installed at the beginning of the furnace and net mass exchange of these masses with flue gases are used to calculate \dot{m}_{IP} based on Eq. (5).

II. Energy balance

Mass flow rates and the thermodynamic properties are the input data used in the energy balance.

- The amount of energy entering into the furnace (\dot{E}_{in}) including four parts, namely, \dot{E}_a , \dot{E}_{NG} , \dot{E}_{GP} , and \dot{E}_{SLP} , is determined with the aid of mass balance performed in section I and measured temperature of each part through using Eqs. (10) to (12).
- The generated energy \dot{E}_{gen} can be calculated by the data

in section I and enthalpy of reaction can be measured by using Eq. (14).

The thermal energy leaving the induration furnace by flue gases, the indurated pellet, cooling water and pallet is determined by the data in section I and Eqs. (17-a) to (17-c) and (19) to (21). In addition, the thermal energy carried away from the furnace by water vapor is easily calculated by Eq. (18). Finally, the waste heat by radiation from the furnace envelope is calculated by using Eq. (22) and employing the furnace surface and temperature.

4- Results and Discussion

Analysis was carried out for a time interval of 5 months, starting on 21 of March, 2015; data were recorded by sensors for every second, resulting in a large volume of the recorded data. To carry out an affordable analysis, data were selected at every three-hour time interval (eight data on each day) from which the daily-averaged values were obtained. It is worth mentioning that some peaks observed in the following figures were due to repair, sudden stop and start of the production line; so, they were excluded from calculations.

Energy and mass flow rates related data were collected by three methods:

- **Pelletizing plant sensors:** the volumetric flow rate of the inlet fresh air, the volumetric flow rate and temperature of the exhaust combustion gases in G5.036, G5.037 and G5.042 ducts, the mass flow rate and temperature of the inlet green pellet and the outlet indurated pellet, the volumetric flow rate of natural gas, and temperature and the volumetric flow rate of the cooling water flow around the furnace body. Data were recorded in the furnace control room every second. It is worth noting that sensors were calibrated once in each year.
- **Laboratory results:** A sample of green and indurated pellets at the entrance and exit of the induration furnace was sent to the laboratory four times a day to determine the weight percentage of sulfur and hematite; also, the water content of green pellets (based on the results of experiments, there was no water in the indurated pellet) was measured. The results of these four samples were averaged and used in the energy analysis.
- **Measuring instruments:** Composition of exhaust flue gases at each duct and walls temperatures were measured by Testo 350, Testo 454 and Testo 881 measuring instruments, respectively. Tables 1 and 2 show the properties of Testo 350, Testo 454 and Testo 881 (Thermal imager) measuring devices, respectively.

The average of three different measurements in the period under investigation at full load operating conditions was used in the calculation. Moreover, measurements by Testo 881 were done in the enclosed environment of the plant and in the absence of wind conditions; hence, the wall temperature variation during the period under the consideration was ignored and was considered constant.

One of the standard methods for doing the uncertainty analysis, is performing various measurements and using them to calculate the standard deviation and average. The composition of flue gases and wall temperature were measured three times in the period under consideration. Although there was a small difference between the measurements in

Table 1. An example of a table

Probe type	Measurement range	Accuracy digit ±1
Temperature measurement	-40 to +1200 °C	±0.5% of mv**
O ₂ measurement	0 to + 25 Vol. % O ₂	0 to 25 Vol.% O ₂
CO ₂	0 to CO ₂ max Vol. % CO ₂	Calculated from O ₂
SO ₂	0 to +5000 ppm SO ₂	±10% of mv
Humidity*	2 to + 31 Vol.% H ₂ O	-----

*Humidity is calculated by Testo 454. **mv: stands for the measured value.

Table 2. Properties of Testo 881 (Thermal imager).

Characteristic	Values	Accuracy
Temperature range	0 - 350 °C	±2 % of reading
Image size	640 × 480 pixels	-----
File format	.bmt	-----

the order of two percent, the average of these measurements was used in calculations. Moreover the mass of magnetite and pyrite which was measured four times each day has a similar difference in four measurements and the average was used in calculations. All the remaining data were measured instantaneously by the sensors calibrated each year and the daily average of these data were employed.

The measured temperatures, mass flow rates and power consumption by the corresponding sensors is instantly sent to the control room. There is an inspection unit in the pelletizing plant that revisits the sensors weekly and send a report to the calibration unit. Some uncertainty in the measurement devices is observed as noise, oscillation and peak in the experimental data. In addition, the iron ore plant has an overhaul each year. During the overhaul, all measuring devices are checked and calibrated. Iranian Environmental Protection Organization (IEPO) has some Trusted Labs. All measurement tools used in these labs must have the calibration certificate from IEPO. The Golgohar company has contracts with some of these labs for the required measurement in the plant. These labs must present calibration certification to the Golgohar company.

The sensors measuring flue gas temperatures are thermocouple of type K which are inspected every month in the calibration unit. These sensors are installed after the electromotor fan at the beginning of each duct. These thermocouples are checked by plotting the thermocouple's voltage-temperature curve by the following instructions:

1. Fill the thermo bath container with water and turn the thermo bath on. Heat the water to 30 degrees Celsius and turn the thermocouple device on. Connect each lead of the multimeter to one end of the thermocouple. This multimeter should be able to measure a voltage of 1 microvolt.
2. Place one junction of the thermocouple into the water and allow the voltage to stabilize. This occurs when the voltage stops fluctuating except for the last digit. Record the stable portion of the voltage from the multimeter.
3. Increase the water temperature to 35 degrees Celsius and record the stable voltage on the multimedia again. Repeat this procedure for each 5-degree increase in temperature from 35 to 60 degrees Celsius.
4. Measure the room temperature and look up the voltage for the thermocouple at the room's temperature. Add this

5. Use the curve-fitting method to find the line that best fits your recorded data. The slope of this line provides the voltage increase for each degree of temperature increase. The voltage on a standard type K thermocouple should increase about 40 microvolts for every degree Celsius increase in temperature.

It should be noted that thermocouples are just checked by the foregoing steps. By observing non-calibration in the thermocouples, they are replaced by new ones. The sensors that measure the temperature of green and indurated pellets are pyrometer infrared thermometer where installed perpendicular to the conveyor carrying the pellets at the beginning and end of the furnace. These sensors are calibrated every six months during overhaul. To this end, by using a thermal imager, the desired temperature is measured and compared with the one of pyrometer infrared thermometer and the difference is determined. A correction factor is inserted in the computer program of the controller when a difference is found and by this method the thermometer is calibrated.

The mass of green and indurated pellets which are carrying by conveyors are measured by load cell schenck instrument. Two methods are used to check this measuring device. 1) The static method in which a specified mass is placed on the conveyor and the readout data is compared by that mass. 2) The dynamic method in which at a specified period (usually one hour) and by knowing the conveyer velocity and using the load cell schenck instrument, the mass flow rate of pellets is measured as tonnage/hour and then this value is compared by the one of a measuring device in the plant and the difference is employed to insert a correction factor to the software of load cell schenck instrument.

The magnetic flow meters are used to measure natural gas mass flow rate which are also compared with those measured by Gas Company each month. It should be noted that due to high quality of these flow meters, they have not calibrated yet.

The mass flow rate of the circulating cooling water is measured by Endress and Hauser Flow meter. A thermosiphon circulating water systems is used in calibration procedure while an accurate and calibrated flow meter is installed and the readout mass flow rate of these devices are compared. Based on their difference, a correction factor is considered for

the controller and flow meter is calibrated. There are a power meter and a sensor for each electromotor. The sensors send the measured energy consumption instantaneously to the control unit. The difference between the energy measured by the power meter and that by the sensor in a period shows the un-calibration of the sensor or the failure of the power meter. It should be noted that the power meter is calibrated on a yearly basis and sensors are checked with them in case they are required to be replaced by new ones.

4- 1- Inlet Green pellet (\dot{m}_{GP})

Operating conditions of the induration furnace were determined based on the conditions of green pellets, which are known as charges and measured by the sensor named tag 101 in Fig. 1. Inlet green pellets contained water and sulfur. Water evaporates and sulfur were oxidized in the furnace. During the conversion of magnetite to hematite, oxygen was absorbed by the pellets and added to the final weight of the indurated pellets. Figure 3 shows the weight of the daily-averaged feed green pellets in tons for the desired period; they were obtained from the measured tonnage of green pellets installed.

4- 2- Determination of the mass and energy flow rate of the inlet fresh air to the induration furnace (\dot{m}_a)

Average outside air temperature, pressure and relative humidity in the Golgohar iron ore pelletizing plant were recorded as 20°C, 82 kPa and 30%, respectively, during the period under consideration. By using these data, air density was obtained to be 0.972 kg/m³ [12]. Fresh air entering into the furnace was used for sealing, combustion and dilution with the volume flow rates of 33143 m³/hr, 16532 m³/hr and 250665 m³/hr, respectively, in addition to the cooling air. Volume flow rate was obtained indirectly through measuring the power consumption of the corresponding fan, the opening percentage of the dampers, and the characteristic curve [11]. It should be mentioned that all dampers were always fully open and fans worked with the maximum power all the time. Therefore, the mass flow rate of the fresh air coming from the three sources mentioned was nearly constant.

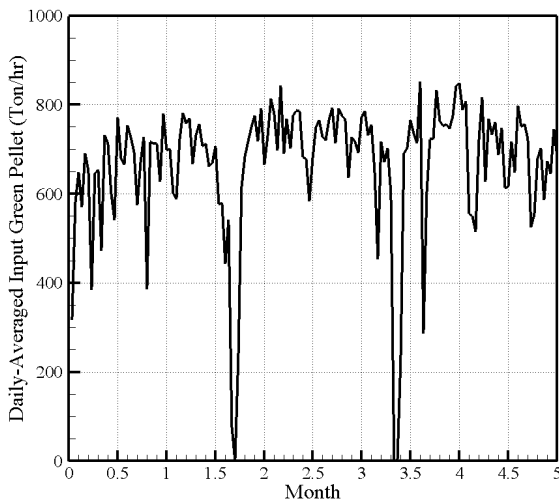


Fig. 3. Daily-averaged input green pellet for the desired period.

The volumetric flow rate of the cooling air was adjusted using an electric fan (G5.002) with the maximum power of 5300 kW. It was obtained based on the fan’s characteristic curve and its power consumption; the results are shown in Fig. 4 in the form of the cooling air volume flow rate based on the daily-averaged values. Variation in the total mass flow of the input fresh air, which was obtained using the air density of 0.972 kg/m³, is shown in Fig. 5 for a period of 5 months. It should be noted that the inlet fresh air was considered at the reference temperature and hence, had no contribution to the inlet energy.

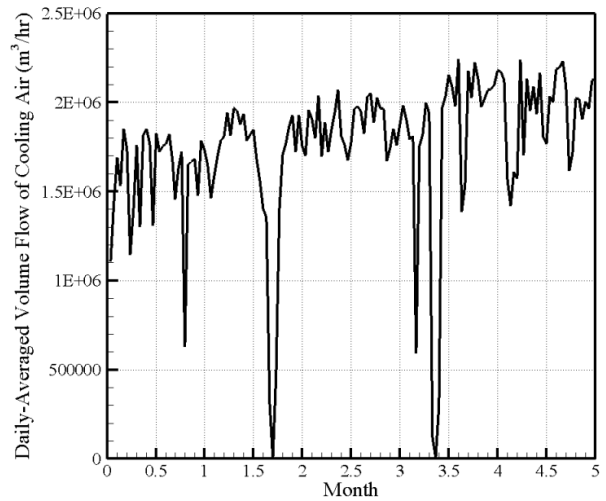


Fig. 4. Variation of the daily-averaged cooling air volume flow rate of the G5.002 fan versus month.

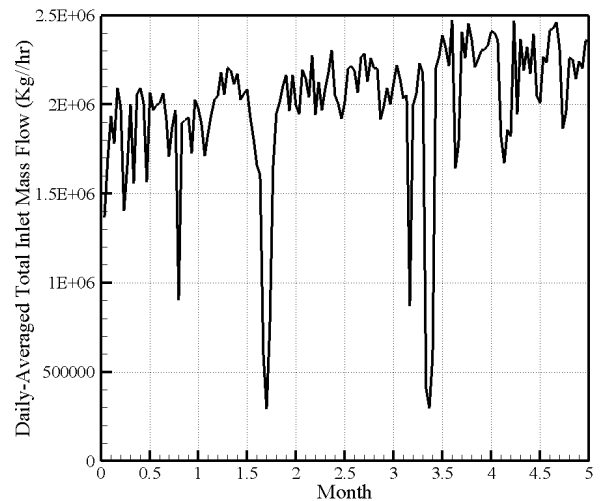


Fig. 5. Variation of the daily-averaged total mass flow rate of fresh air versus month.

4- 3- Energy generation in the induration furnace (\dot{E}_{gen})

Heat is generated in the induration furnace through natural gas burning (\dot{E}_{NG}), conversion of magnetite to hematite (\dot{E}_{Feo}) and pyrite burning (\dot{E}_{pyrite}). The high heating value of natural gas is 8600 kCal/Nm³ in the standard conditions. As there was enough oxygen in the process, the complete combustion of natural gas occurred. Fig. 6 (a) shows the daily-averaged

natural gas energy production as obtained by multiplying the amount of the natural gas consumption by the gas heating value (Eq. (14)). An installed flow meter measured the natural gas consumption in the normal cubic meter. The most important process in the induration furnace was the oxidation of magnetite to hematite in the iron ore pellets. During this exothermic reaction, an amount of energy equal to $\Delta H = -513 \text{ kJ/kg (Fe}_3\text{O}_4)$ was released. It is worth mentioning that the weight of the reacted magnetite in the process was equal to the difference between the magnetite weight of green and indurated pellets. Thermal energy released in the process came from this reacted magnetite (see Eq. (14)). Fig. 6 (b) displays the daily-averaged energy production for the period under consideration.

Sulfur content in the inlet green pellets was in the form of iron sulfide (pyrite). The difference between the weight of sulfur in green and indurated pellets was equal to the weight of the burned sulfur in the process. Roasting of sulfides in an exothermic reaction is represented by $\text{FeS}_2 + 11\text{O}_2 \rightarrow 2\text{Fe}_2\text{O}_3 + 8\text{SO}_2$, with the heat generation of

$\Delta H = -6943 \text{ kJ/kg (FeS}_2)$. Fig. 6 (c) shows the daily-averaged energy generated for the period under consideration; it was obtained from the product of pyrite mass flow rate and the released energy in this reaction (see Eq. (14)). Heat is generated in the induration furnace as a result of natural gas burning, conversion of magnetite to hematite, and burning of pyrite. Variation of the daily-averaged total generated thermal energy in the pelletizing plant is shown in Fig. 6 (d) (see Eq. (13)). It can be seen that most of the generated energy was by magnetite and pyrite, which supplied the required energy for pellet induration, leading to the reduction in the natural gas consumption.

The two pulsed reductions shown in Fig. 3 and 6 (a) correspond to the periods of no production. Even though nothing was charged into furnace during these periods, some burners were turned on to prevent the generation of thermal stress while keeping furnace warm. It should be noted that the energy content of the inlet natural gas was not considered in energy calculations as it was at the reference temperature.

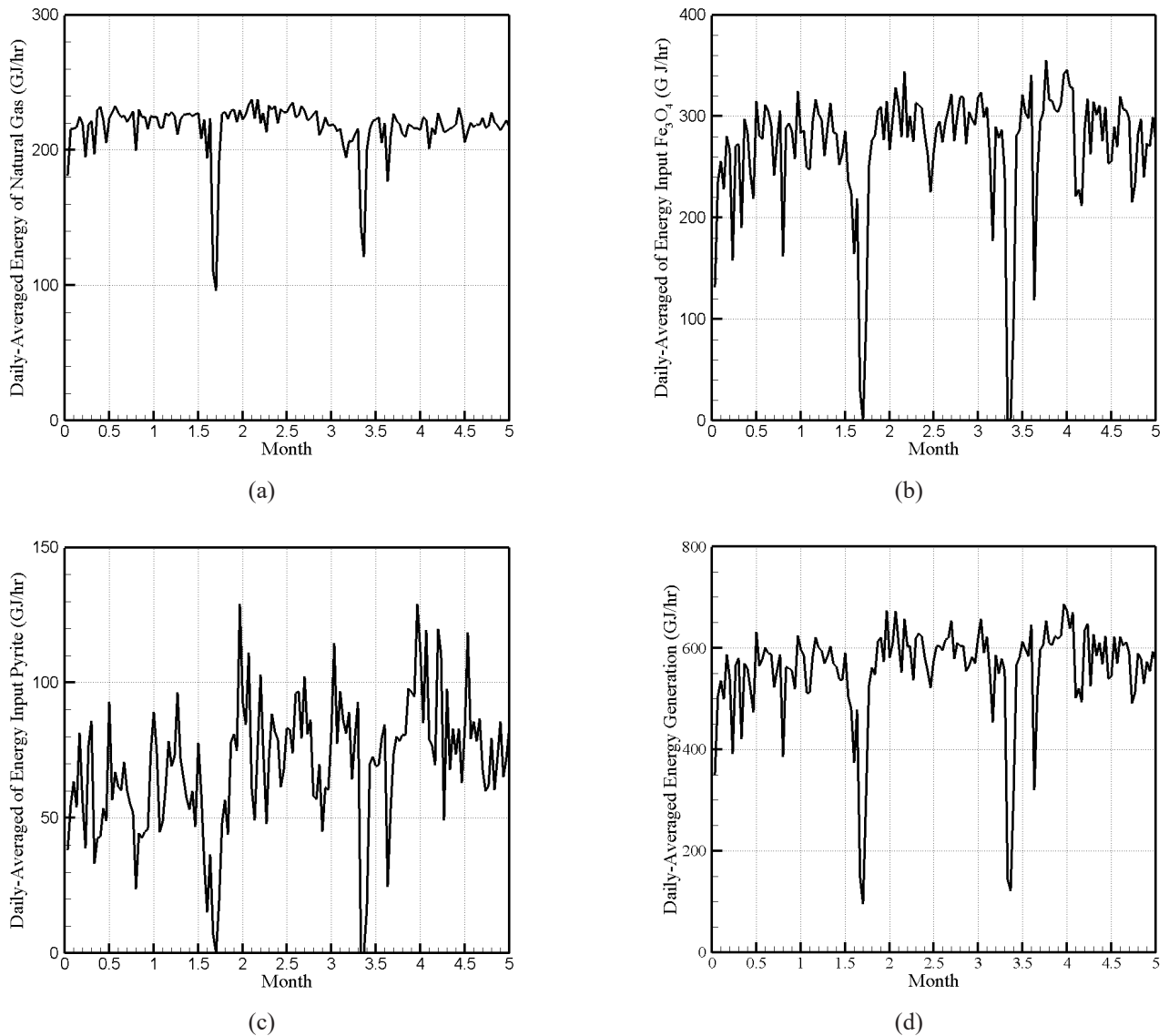


Fig. 6. Daily-averaged heat generation by (a) burning natural gas, (b) oxidation of magnetite to hematite, and (c) pyrite burning, with (d) their summation in the pelletizing plant for the period under investigation.

4- 4- Energy leaving the induration furnace (\dot{E}_{out})

Thermal energy is transferred from the induration furnace by various means including flue gas flow in the three ducts of the plant, the latent heat of water vapor, energy storage by the indurated pellets, pallets and cooling water, and the emitted radiation from the furnace body. Contribution of each sector to the total waste heat energy is discussed in detail in the following sections.

4- 4- 1- Thermal energy transferred by exhaust flue gases (\dot{E}_{FG})

Exhaust flue gases entered into main stack through three ducts. Flue gases in these ducts had different compositions and temperatures. Components of the exhaust gases at each duct were measured by the Testo 350 gas analyzer. This device measures volume fractions of the flue gas components and converts them in to the mass percentage by thermodynamics relations [12]. Table 3 displays the mass percentage of the flue gas components in the three ducts.

As can be observed in this table, other gases (last column) comprised less than 1% of flue gases and therefore, could be ignored in the present analysis. The daily-averaged flue gas mass flow rate of each duct could be obtained by using the power consumption of the driving motors of fans, the opening percentage of dampers, and the characteristic curves of fans. The energy consumption of the electro motors was continuously recorded by the sensors. In addition, the volumetric flow rate of flue gases was obtained using the characteristic curves. Owing to the variable temperature of flue gases in each duct, flue gas density was not constant and could be obtained for each day. Fig. 7 shows variation in the mass flow rate for each duct.

Comparison of the mass flow rate for the inlet air and the outlet flue gases showed a difference of less than three percent, due to the chemical reactions of pyrite burning and conversion of magnetite to hematite, as well as water vapor. This could be observed in Fig. 8, which shows the ratio of the exhaust flue gases to the inlet fresh air.

Due to the importance of flue gas temperature in waste heat recovery, as measured by sensors installed after each fan, the temperature at the outlet of three ducts is presented in Fig. 9 for the period under study. It could be observed that the flue gas temperature of duct G5.037 was considerably higher than that of the other two ducts.

By knowing the temperature and the mass flow rate of flue gas at each duct, the sensible thermal energy could be calculated. The density and specific heat are temperature dependent and should not be considered constant, with a noticeable temperature change occurring in the furnace. In this study, the density and specific heat capacity were calculated from the known correlations [12] at different locations (boundaries) which had different temperatures. Moreover, at each location, there was temperature variation during the period under consideration. Hence, based on the aforementioned temperature variations, this point was considered in all

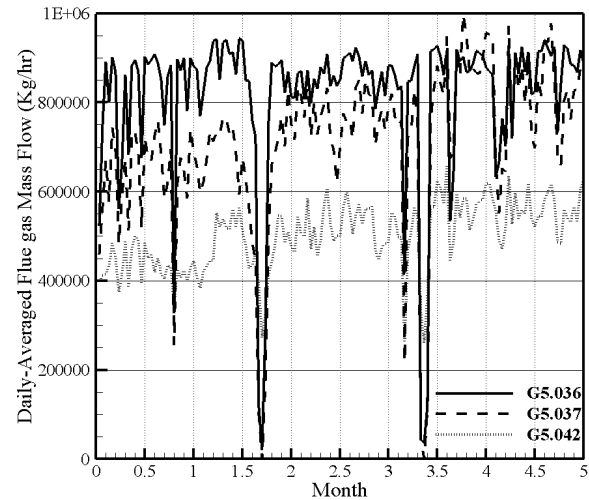


Fig. 7. Variation of the daily-averaged mass flow rate of flue gas versus month.

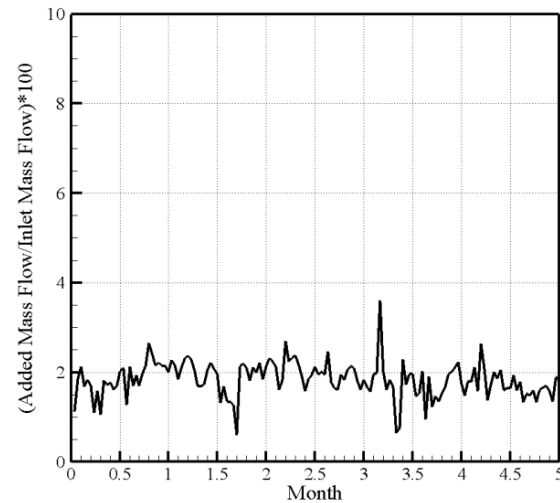


Fig. 8. Variation in the ratio of the added mass flow rate to the inlet mass flow rate versus month

calculations. Finally, by using Eq. (17) and Figs. 7 and 9, the flow gas sensible energy could be obtained. Variation in the daily-averaged flue gas sensible energy at the outlet of the three ducts is shown in Fig. 10. As can be observed in Figs. 9 and 10, the quality and quantity of the energy of flue gases leaving the duct G5.037 were the highest among the three ducts. Energy quality is of prime importance in heat recovery devices.

4- 4- 2- Latent heat of water vapor (\dot{E}_{wv})

By measuring humidity using Testo 454 and thermodynamics relations [12], the water content at each duct could be

Table 3. Mass percentage of the flue gas components in the three ducts.

Gas Component	N ₂ %	O ₂ %	H ₂ O%	CO ₂ %	SO ₂ %	Other gases%
Duct G5.036	74	20.78	3.45	0.55	0.22	<1
Duct G5.037	76	17.4	3.6	0.8	1.2	<1
Duct G5.042	74.8	21.3	2.63	0.21	0.06	<1

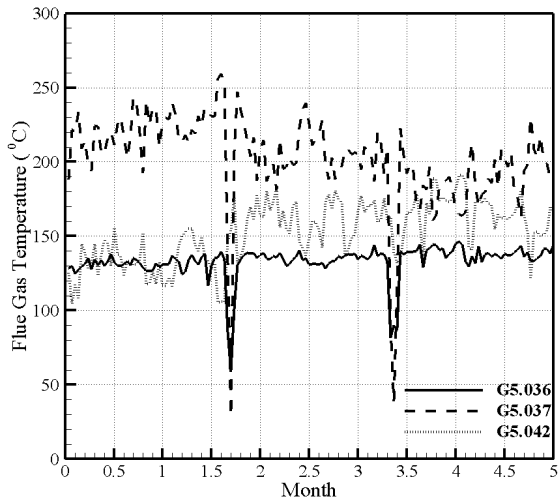


Fig. 9. Variation in the daily-averaged flue gas temperature at the three ducts outlet versus month.

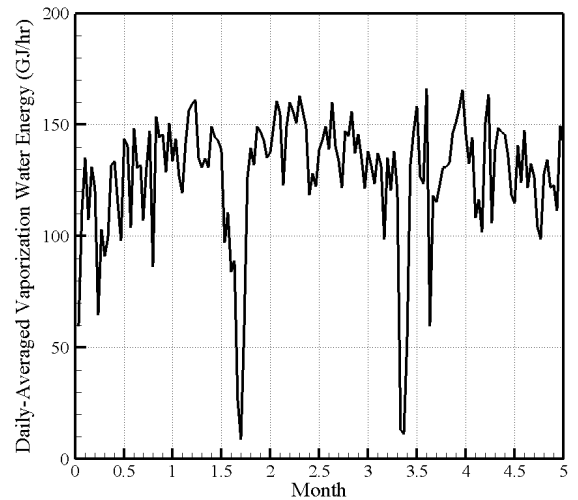


Fig. 11. Variation in the daily-averaged energy carried by water vapor at three ducts versus month.

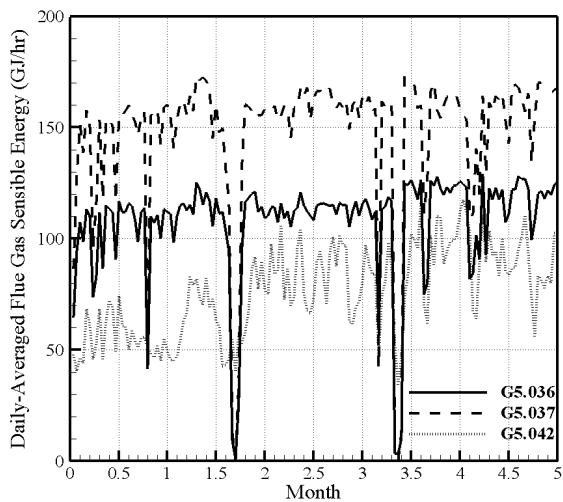


Fig. 10. Variation in the daily-averaged flue gas sensible energy at the three ducts outlet versus month.

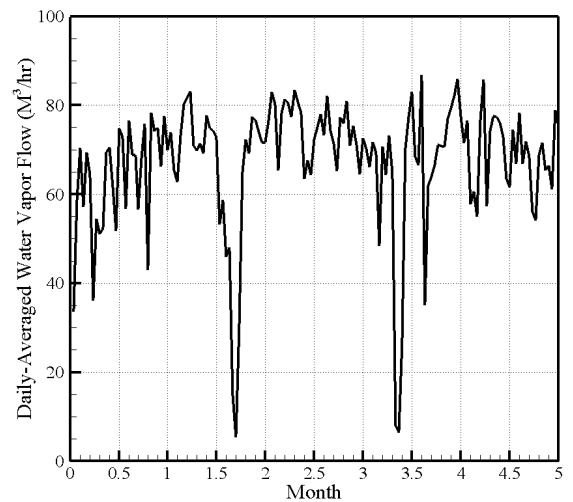


Fig. 12. Variation in the daily-averaged mass flow rate of water vapor at the stack outlet versus month.

determined. Water content of the inlet green pellets fed into the furnace was between 5% to 9% of its total weight, as determined by averaging the laboratory data measured four times each day. During the up-draught, down-draught and preheating stages in the induration furnace, this water was vaporized. As another source, combustion of natural gas produced water vapor. This water vapor entered into the flue gases. The amount of energy carried by water vapor was determined by multiplying the vapor mass flow rate and the latent heat, which was considered to be 2.25 MJ/kg in this energy analysis. Fig. 11 shows the daily-averaged variation of this energy at each duct for the time period under consideration. This process took place in the up-draught, down-draught and preheating stages with the dominant one being the up-draught stage.

In addition, the combustion of natural gas at the end of preheating and firing stages generated water vapor as a combustion by-product. Adding these two amounts of water vapor produced at each stage revealed that the duct No. G5.037 contained the maximum water vapor, as compared

to the other two ducts. It should be mentioned that the inlet fresh air contained some water vapor. This water vapor left the furnace without any change. Three sources of water vapor in the furnace were water vapor produced by the vaporization of water content in the green pellets, natural gas reaction, and the inlet fresh air entering the main stack. Fig. 12 depicts the variation in the daily-averaged mass flow rate of water vapor at the stack outlet.

4-4-3- Energy stored in the materials (\dot{E}_{IP} , \dot{E}_{pallet} and \dot{E}_{CW})

Thermal energy leaving the induration furnace occurred in the form of stored energy in the indurated pellets, pallets and cooling water.

4-4-3-1- Indurated pellets

About one fourth of the inlet pellets was in the form of indurated pellets (side layer pellet). It should be noted that installed sensors at the end of furnace recorded the temperature and the mass flow of the indurated pellets, which were displayed in the control room. By knowing these data

and the heat capacity of the indurated pellets, the stored energy in the indurated pellets was calculated. The indurated pellets returning into furnace by a rail and green pellets had the temperature of (approximately) 80°C and 45°C, respectively. Based on these values, the average temperature for the whole inlet pellets (green and indurated) was obtained to be 55°C. The average heat capacity of the indurated pellets was 0.586 J/kg.K. Fig. 13 displays the net variation of the daily-averaged outlet energy by the indurated pellets (the difference between Eqs. (12) and (19)).

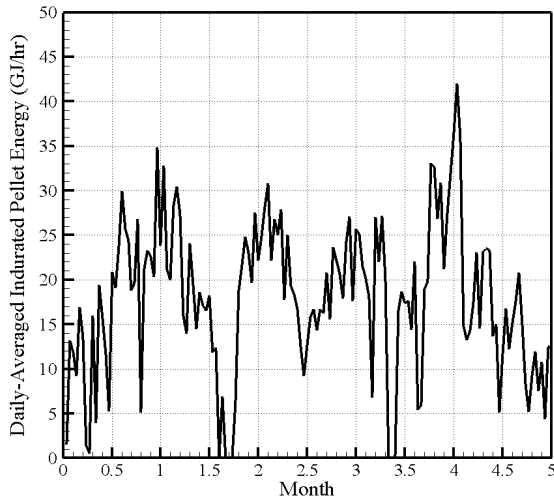
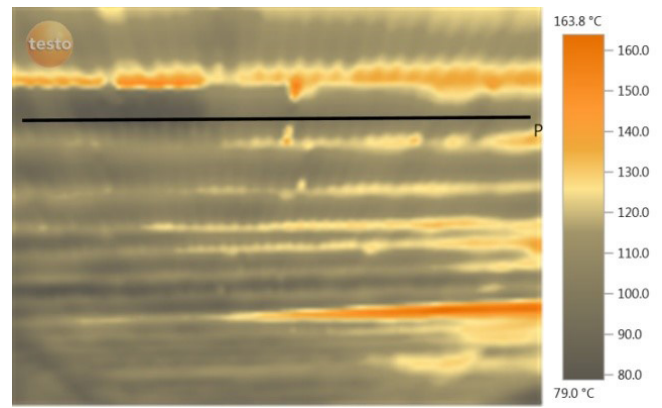


Fig. 13. Variation in daily-averaged outlet energy by the indurated pellets versus month.

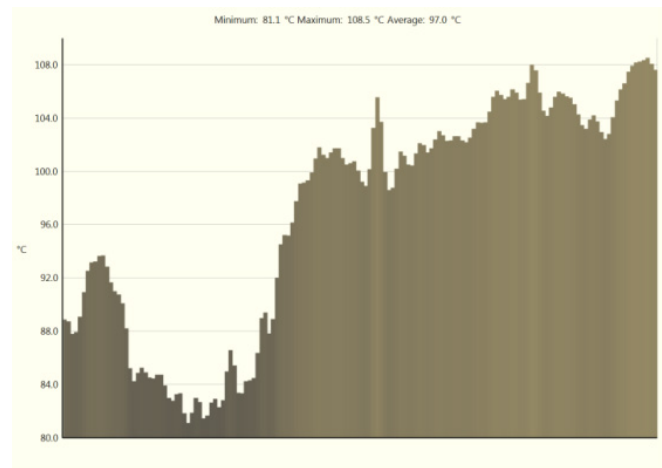
4- 4- 3- 2- Pallets

The grate bars (pallets) conveying the pellets to the end of the furnace left the induration furnace and then came back to the beginning of the furnace. During the return path, the pallets were exposed to the environment and its temperature was decreased, leading to the loss of its stored energy. Speed and thermal capacity of the pelletizing rail carriers (pallets) were 4.2 m/min and 0.45 kJ/kg.K, respectively. According to the pallet speed and the length of the pellet (1.5 m), 168 pallets were cooled during the one-hour operation. Hence, the total weight of the cooled pallets was 1680000 kg.

Fig. 14 (a) is a picture of the furnace body in which a black straight line can be seen. Fig. 14 (b) shows the temperature distribution throughout this line and hence, these figures are shown together. To illustrate the temperature distribution in the width of the grate pallet, two images were taken by a thermal camera (Testo 881) from the beginning (Fig. 14 (a)) and end (Fig. 15 (a)) of the rail carrier pellets and imported to the Testo software. By drawing a line on these photos, the temperature distribution in the width of the grate pallet was determined. In Figs. 14 (a) and 15 (a), which are pictures of the furnace body, there are black straight lines. Figs. 14 (b) and 15 (b) depict temperature distribution along these black lines. As can be seen, the average temperature of the pallet at the furnace inlet and outlet was 97 °C and 147.4 °C, respectively. The average temperature was about 50°C, resulting in an energy loss of approximately 38 GJ/hr (see Eq. (21)).



(a)



(b)

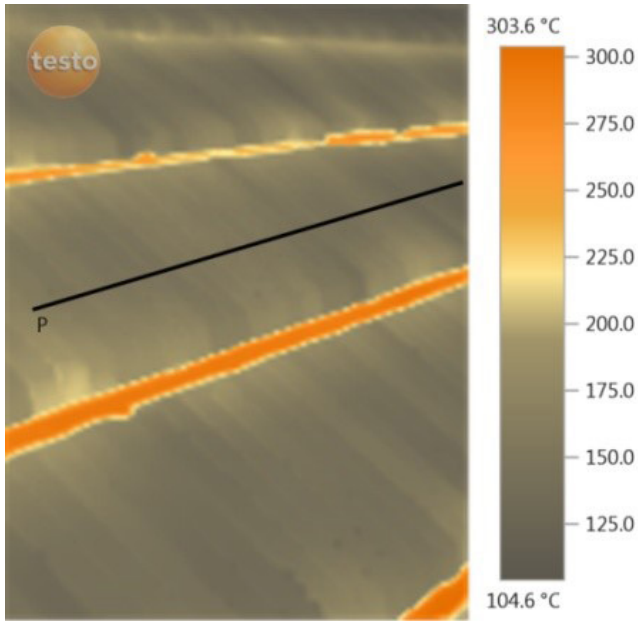
Fig. 14. Temperature distribution in the width of the grate pallet: (a) Furnace inlet, and (b) software analysis.

4- 4- 3- 3- Cooling water

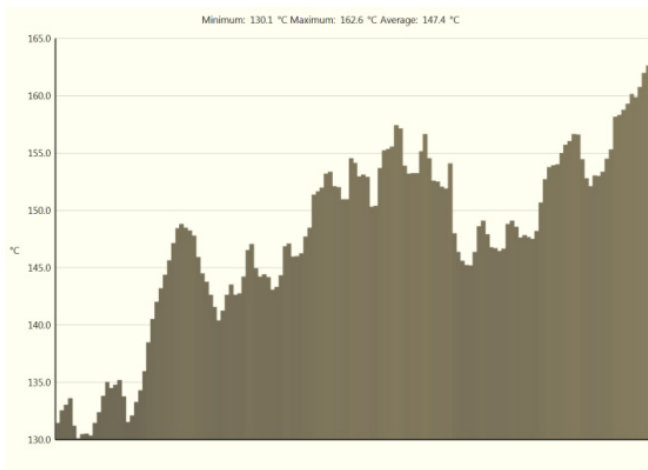
Thermal energy was exhausted from the induration furnace by cooling water, which circulated around the furnace body. This cooling water, which absorbed the sensible heat of oil used in the lubrication system, had the volumetric flow rate of 370 m³/hr. In addition, the difference between the inlet and outlet water temperature was about 7 °C, on average. Figure 16 displays the variation in the daily-averaged heat removal by cooling water, according to Eq. (20).

4- 4- 4- The contribution of the emitted radiation from the furnace body (\dot{E}_{rad})

Measurements by Testo 881 were done in the enclosed environment of the plant and in the absence of wind conditions; hence, the wall temperature variation during the period under the consideration was ignored. According to the images taken by the thermal camera (Testo 881), the average temperature of the furnace body was about 115 °C; therefore, waste heat in the form of thermal radiation was expected to occur. Furnace body, which had been made from stainless steel, had the surface area of 3500 m² and the emissivity of 0.7. Fig. 17 shows the temperature distribution of different parts of the induration furnace. The surface area consisted of hoods containing hot gases (Fig. 17 (a)) as the dominant area, connections (Fig. 17 (b)), furnace walls (Fig. 17 (c)), and burner body (Fig. 17 (d)). The effect of wind on the heat



(a)



(b)

Fig. 15. Temperature distribution in the width of grate pallet: (a) Furnace outlet, and (b) software analysis.

transfer was ignored as the furnace was enclosed in another one. The energy loss from the furnace body by radiation was obtained using Eq. (22). The total rate of energy dissipation from the furnace was about 14 GJ/hr.

To summarize, Tables 4 and 5 show the daily-averaged contribution of each sector of the induration furnace to the thermal energy production and consumption for the period under consideration (from 21 of March to 22 of August, 2015). As could be observed from Table 5, contribution of other losses was 40 (GJ/hr) or 7.19 percent of the energy

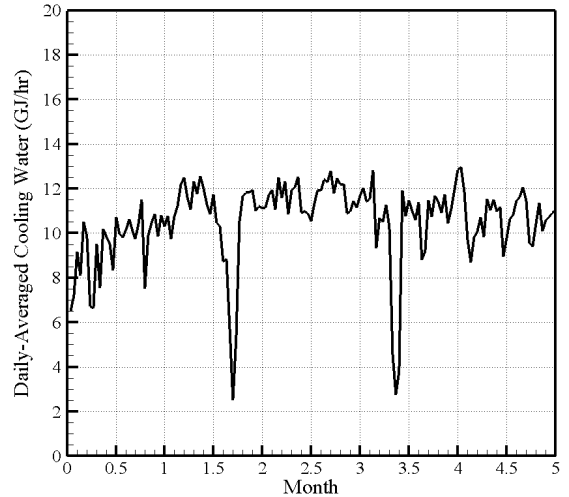


Fig. 16. Variation in the daily-averaged heat removal by cooling water versus month.

produced. These losses could be due to the air leakage from the furnace because of defects, air aspiration inside the furnace because of the negative pressure in some sections of the furnace, water crystals in the green pellets compounds that needed energy to evaporate [11], and free convection heat transfer of the furnace body.

As can be observed from Table 5, the portion of the heat exhaust from furnace by flue gases in the form of sensible and latent heat was 55.51% and 22.33% respectively, resulting in a total waste heat of 78.34%. This was a considerable amount of heat (at least) part of which might be recovered using a proper waste heat recovery method. Currently, authors are working on waste heat recovery from these flue gases through the design of a proper heat exchanger to produce the required heat for the operation of a Multi Effect Desalination (MED) system used for producing fresh water from salt water.

5- Conclusion

In the present study, the mass and energy analysis of the Golgohar iron ore pelletizing plant was carried out for a period from 21 March 2015 to 22 August 2015. The sources of energy production were the burning of natural gas, conversion of magnetite to hematite, and the burning of pyrite. On average, the contribution of these to the total produced energy was 38.99%, 48.51%, and 12.5%, respectively. It was observed that the main portion of the energy production (61.01%) was obtained from the reactions in the furnace. It should be noted that the G5.002 fan, which brought the fresh air into the furnace to cool the indurated pellets, was heated and used in up-draught, down-draught, preheating, and firing processes. Furthermore, it was observed that energy leaves the furnace via flue gases in three ducts of the plant, indurated pellets, pallets, and cooling water, as well as the

Table 4. The daily-averaged contribution of the energy production of the induration furnace, from 21 of March to 22 of August, 2015.

Heat generated by	Energy production, GJ/hr	Energy production, %
Natural gas burning	217	38.99
Oxidation of magnetite to hematite	270	48.51
Pyrite burning	69.5	12.5
Total	556.5	100

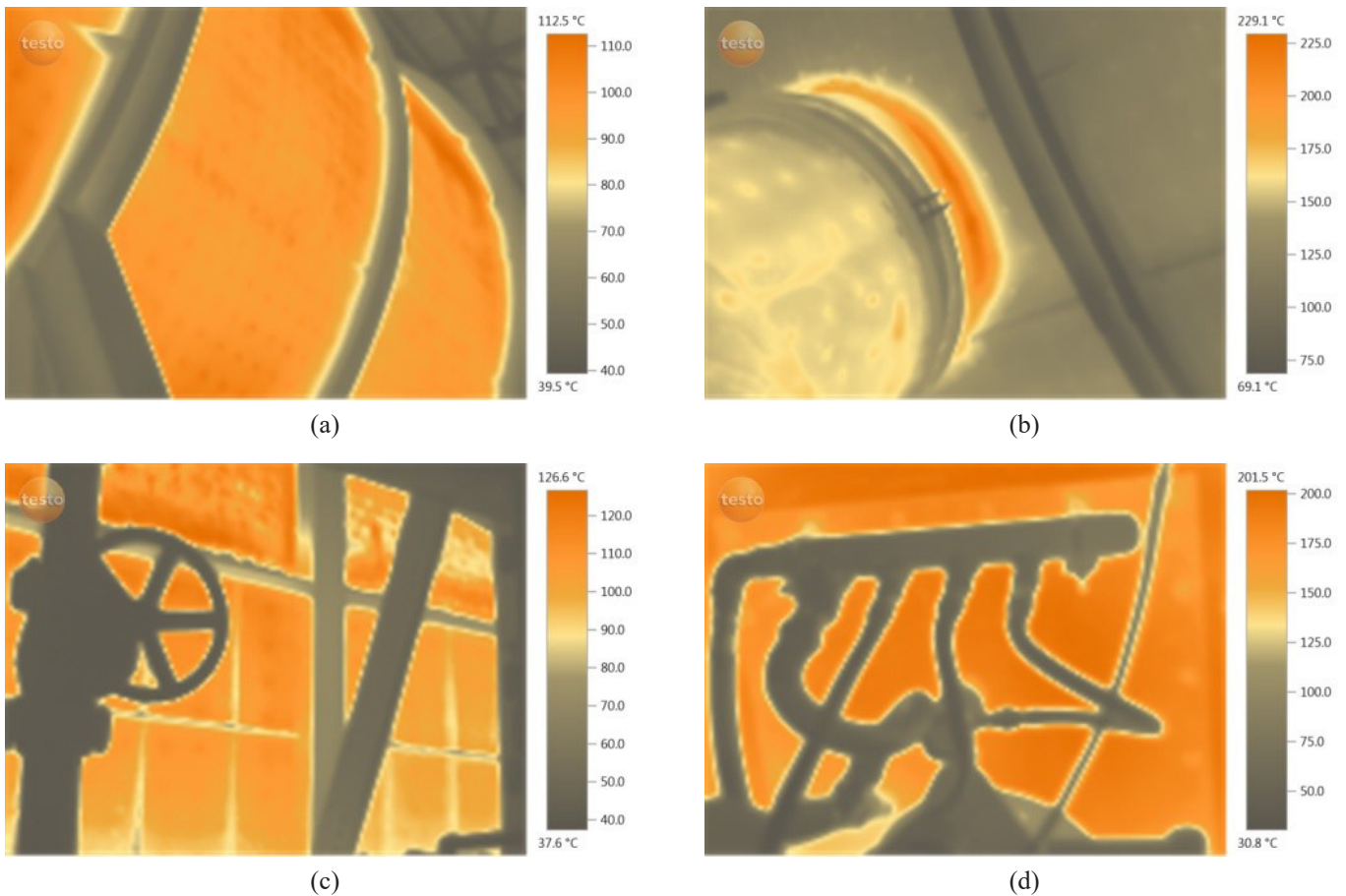


Fig. 17. Temperature distribution of different parts of the induration furnace: (a) Hot gases transmission line (Hood), (b) Connections, (c) Furnace walls, and (d) Burner body.

Table 5. Daily-averaged contribution of the energy consumption of the induration furnace, from 21 of March to 22 of August, 2015

Heat removed		Energy removed, GJ/hr	Percent (%)
Flue gas (Sensible)	Duct G5.036	98.6	17.72
	Duct G5.037	140.1	25.19
	Duct G5.042	70.3	12.6
Water vaporization (Latent)	Duct G5.036	24.25	4.35
	Duct G5.037	53.93	9.7
	Duct G5.042	48.82	8.78
Storage	Rail pallets	38	6.83
	indurated pellets	18	3.24
	Cooling water	10.5	1.89
Emitted radiation		14	2.51
Imbalance		40	7.19
Total		556.5	100

emitted radiation from the furnace body. Besides, energy analysis in the considered control volume showed that the main part of the exhaust energy of the furnace was from flue gases in three ducts containing the sensible and latent heat. This part comprised the dominant portion of the waste heat, which was about 78%. The results revealed that both energy quantity and quality of the duct No. G5.037 were the highest among three ducts. Contribution of other losses were found to

be about 7.19 percent. Owing to the fact that the reactions in the induration furnace are exothermic, more than 60 percent of the required energy for the process was supplied by the oxidation of magnetite to hematite and pyrite burning. The results obtained in this study could be used as the input data for designing a heat exchanger producing vapor for thermal desalination methods such as multi effect distillation (MED), etc. Moreover, the results could be employed for

the power generation cycles run by waste heat, such as the organic Rankine and kalina cycle. The authors are using these results in an ongoing study for water desalination by a MED method. The readerships can also can make use of the present results for the mentioned power generation cycles.

Acknowledgment

This work was financially supported by Golgozar Iron Ore and Steel Research Institute, Golgozar Mining and Industrial Company, Sirjan, Iran, with project No: 60907894/94-121.

Nomenclature

A	Heat transfer area, ft ²
C_p	Specific heat at constant pressure (kJkg ⁻¹ K ⁻¹)
E	Energy rate (MJhr ⁻¹)
H	Enthalpy of formation (kJkg ⁻¹)
m	Mass flow rate (kghr ⁻¹)
T	Temperature (°C, R)
V	Wind velocity (ms ⁻¹ , fts ⁻¹)

Greek symbols

ε	emissivity
Δ	Difference

Abbreviations

a	air
BCA	Burner Combustion Air
CA	Cooling Air
Conv.	Convection
CW	Cooling Water
DA	Dilution Air
DP	Drying Pellet
FG	Flue Gas
GP	Green Pellet
IP	Indurated Pellet
NG	Natural Gas
Rad	Radiation
Ref	reference
SA	Sealing Air
SLP	Side Layer Pellet
Sur	Surface
WV	Water Vaporization

Subscripts

Gen	generation
In	Inlet
Out	Outlet

References

- [1] S. Brückner, S. Liu, L. Miró, M. Radspieler, L. F. Cabeza, E. Lävemann, Industrial waste heat recovery technologies: an economic analysis of heat transformation technologies, *Applied Energy*, 151 (2015) 157-167.
- [2] S. Brueckner, L. Miró, L. F. Cabeza, M. Pehnt, E. Laevemann, Methods to estimate the industrial waste heat potential of regions—A categorization and literature review, *Renewable and Sustainable Energy Reviews*, 38 (2014) 164-71.
- [3] F. Vitoretti, J. A. De Castro, Study of the induration phenomena in single pellet to traveling grate furnace, *Journal of Materials Research and Technology*, 2 (2013) 315-322.
- [4] S. Majumder, P. V. Natekar, V. Runkana, Virtual indurator: A tool for simulation of induration of wet iron ore pellets on a moving grate, *Computers and Chemical Engineering*, 33 (2009) 1141-1152.
- [5] M. Barati, Dynamic simulation of pellet induration process in straight-grate system, *International Journal of Mineral Processing*, 89 (2008) 30-39.
- [6] J. x. Feng, Y. Zhang, H. w. Zheng, J. h. Xu, Y. m. Zhang, J. b. Yang, Optimization of pellet production process parameters in grate using simulation results, *Journal of Shanghai Jiaotong University (Science)*, 16 (2011) 219-223.
- [7] S. Nordgren, J. Dahl, C. Wang, B. Lindblom, Process integration in an iron ore upgrading process system: analysis of mass and energy flows within a straight grate induration furnace, 18th *International Congress of Chemical and Process Engineering*, (2008).
- [8] S. Sadrnezhaad, A. Ferdowsi, H. Payab, Mathematical model for a straight grate iron ore pellet induration process of industrial scale, *Computational Materials Science*, 44 (2008) 296-302.
- [9] J. Feng, Y. Zhang, H. Zheng, X. Xie, C. Zhang, Drying and preheating processes of iron ore pellets in a traveling grate, *International Journal of Minerals, Metallurgy and Materials*, 17 (2010) 535-40.
- [10] Process Equipment List pelletizing Plant 5.0 Million ton per day, (2006) 1- 403.
- [11] Pelletizing Plant 5.0 Million ton per day Operating Manual, (2006) 1- 196.
- [12] V. Wylen, J. Gordon, R. E. Sonntag, *Fundamentals of Thermodynamics* 6th Edition, New York: Wiley, (2002).
- [13] V. Chanapathy, *Find surface heat loss and flue gas density quickly*, Hydrocarbon Process (United States), (1985) 64.
- [14] V. Arora. *Check fired heater performance*, Hydrocarbon Process (United States), (1985), 64-65.

Please cite this article using:

S. Goodarzi, E. Jahanshahi Javaran, M. Rahnama, M. Ahmadi, Estimation of Waste Heat from Exhaust Gases of an Iron Ore Pelletizing Plant in Iran, *AUT J. Mech. Eng.*, 2(2) (2018) 263-276.

DOI: 10.22060/ajme.2018.14151.5707

